Journal of Solid State Chemistry 182 (2009) 932–941

Contents lists available at ScienceDirect

Journal of Solid State Chemistry

journal homepage: www.elsevier.com/locate/jssc

Mild hydrothermal synthesis, crystal structure, thermal behavior, spectroscopic and magnetic properties of the $(NH_4)[Fe(AsO_4)_{1-x}(PO_4)_xF]$ ($x = 0.3$, 0.6, 0.8) series. Thermal transformation of $(NH_4)[Fe(AsO_4)_{0.7}(PO_4)_{0.3}F]$ into the textural porous orthorhombic $Fe(AsO_4)_{0.7}(PO_4)_{0.3}$

Teresa Berrocal [a], José L. Mesa [b,*], José L. Pizarro [a], Begoña Bazán [a], Luis Lezama [b], María I. Arriortua [a], Teófilo Rojo [b]

[a] Departamento de Mineralogía y Petrología, Facultad de Ciencia y Tecnología, Universidad del País Vasco/EHU, Apdo, 644, E-48080 Bilbao, Spain
[b] Departamento de Química Inorgánica, Facultad de Ciencia y Tecnología, Universidad del País Vasco/EHU, Apdo, 644, E-48080 Bilbao, Spain

ARTICLE INFO

Article history:
Received 3 November 2008
Received in revised form
15 January 2009
Accepted 16 January 2009
Available online 1 February 2009

Keywords:
Mild hydrothermal synthesis
Iron(III) arsenates–phosphates
Crystal structure
IR and UV–Vis spectroscopies
ESR
Magnetism

ABSTRACT

The $(NH_4)[Fe(AsO_4)_{1-x}(PO_4)_xF]$ ($x = 0.3$, 0.6, 0.8) series of compounds has been synthesized under mild hydrothermal conditions. The compounds crystallize in the orthorhombic $Pna2_1$ space group, with the unit-cell parameters $a = 13.1718(1)$, $b = 6.5966(6)$, $c = 10.797(1)$ Å for $x = 0.3$; $a = 13.081(1)$, $b = 6.5341(6)$, $c = 10.713(1)$ Å for $x = 0.6$ and $a = 13.0329(9)$, $b = 6.4994(4)$, $c = 10.6702(6)$ Å for $x = 0.8$, with the volumes 938.6(1), 915.7(1) and 903.8(1) Å^3, respectively, with $Z = 8$. Single crystals of $(NH_4)[Fe(AsO_4)_{0.7}(PO_4)_{0.3}F]$ heated under air atmosphere at 465 °C remain as single crystals, changing the composition to $Fe(AsO_4)_{0.7}(PO_4)_{0.3}$. This later phase belongs to the orthorhombic *Imam* space group, with the unit cell parameters $a = 13.328(2)$, $b = 6.5114(5)$, $c = 10.703(1)$ Å, $V = 928.9(2)$ Å^3 and $Z = 12$. The crystal structure of the ammonium phases consists of a KTP three-dimensional framework constructed by chains formed by alternating $Fe(2)O_4F_2$ or $Fe(1)O_4F_2$ octahedra and $As/P(2)O_4$ or $As/P(1)O_4$ tetrahedra, respectively. These octahedra and tetrahedra are linked by a common oxygen vertex. The chains run along the "*a*" and "*b*" crystallographic axes. The crystal structure of $Fe(AsO_4)_{0.7}(PO_4)_{0.3}$ is a three-dimensional skeleton derived from that of the precursor, formed from (100) sheets stacked along the [001] direction, and interconnected by chains of alternating $Fe(2)O_6$ octahedra and $As/P(2)O_4$ tetrahedra sharing a vertex in the "*a*" direction. Transmission electronic microscopy of this compound indicates the existence of unconnected external cavities with a BET surface area of 3.91(3) m^2 g^{-1}. The diffuse reflectance spectra in the visible region show the forbidden electronic transitions characteristic of the Fe(III) d^5-high spin cation in slightly distorted octahedral geometry, for all the compounds. The ESR spectra for all the compounds, carried out from room temperature to 4.2 K, remain isotropic with variation in temperature; the *g*-value is 1.99(1). Magnetic measurements indicate the predominance of antiferromagnetic interactions, with Néel temperatures near to 70.0 and 50.0 K for the ammonium phases and $Fe(AsO_4)_{0.7}(PO_4)_{0.30}$, respectively. At low temperatures a spin canting phenomenon for $Fe(AsO_4)_{0.7}(PO_4)_{0.30}$ is detected.

1. Introduction

The research on phosphate, phosphite and arsenate compounds with new open frameworks is currently in progress due to their potential applications in catalysis, gas separation or as ion exchange [1,2]. Among the many open-framework compounds known, those based on the phosphate oxoanion appear to be the dominant class [1,3,4]. In addition to the use of tetrahedral phosphate groups as building units, other anionic moieties such as borates [5], arsenates [6], sulphates [7] and selenates [8] have been used successfully in the preparation of novel open-framework structures. Of these, the arsenates are interesting because, although arsenic belongs to the same group of the periodic table as phosphorous, the larger size of the $(AsO_4)^{3-}$ anion can give rise to different structures and/or physical properties. Thus, many arsenate frameworks of different structure and composition have been prepared and characterized [6,9–15]. Furthermore, addition of fluoride anions into the reaction mixture,

* Corresponding author. Fax: +34 946013500.
E-mail address: joseluis.mesa@ehu.es (J.L. Mesa).

0022-4596/$ - see front matter © 2009 Elsevier Inc. All rights reserved.
doi:10.1016/j.jssc.2009.01.026

developed by Guth, Kessler and Ferey [16], has led to the discovery of new microporous structural types, some of them exhibiting very large channels such as in cloverite [17], ULM-5 [18], MIL-31 [19], MIL-46 [20] and VSB-5 [21]. In these phases, the fluorine anions are linked in the coordination sphere of the metal cation. A systematic study of the fluorine systems [22] has shown that the geometry of the structure-directing agent plays an important role for the attainment of a three-dimensional open framework. It has also been observed that the ammonium groups from the organic molecules preferentially interact with the fluorine atoms of the framework via hydrogen bonds.

In recent years, to establish the relationships between the templates and the inorganic framework, the scientists working in this research field have focused their attention on nitrogen rich molecules, such as ethylenediamine, 1,3-diaminopropane, piperazine, 1,4-diazabicyclo[2.2.2]octane, 1,4,8,11-teraazacyclotetradecane, etc. [23]. In these organically templated compounds the crystal structure collapses after losing the organic cation under heating. However, precursor materials with an open framework containing building units, such as the ammonium cations, inside the inorganic skeleton, could provide a new synthetic route to obtain new condensed phases by thermal treatment of these kinds of precursor. Furthermore, the use of both the ammonium cation and the fluoride anion together with an appropriate synthetic procedure could favor the attainment of new porous materials after thermal treatment of the resulting precursor. In this way, we have recently synthesized the new orthorhombic *Imam* $Fe(AsO_4)$ phase that exhibits a condensed structure with textural porosity [24]. This arsenate has been prepared as single crystals by heating single crystals of the $(NH_4)[Fe(AsO_4)F]$ precursor, which allows to the elimination of $(NH_4)F$. However, the $(NH_4)[Fe(PO_4)F]$ phosphate [25] does not exhibit this kind of thermal behavior.

In this work we report on the mild hydrothermal synthesis of the $(NH_4)[Fe(AsO_4)_{1-x}(PO_4)_xF]$ ($x = 0.3$, 0.6, 0.8) series of compounds with $KTiO(PO_4)$-type structure [26]. Its thermal behavior has been investigated, and it has been found that the $(NH_4)[Fe(AsO_4)_{0.7}(PO_4)_{0.3}F]$ composition yields the new mixed $Fe(AsO_4)_{0.7}(PO_4)_{0.3}$ phase that also exhibits textural porosity. In addition, it has been deduced that increasing the (PO_4) fraction in the composition of the $(NH_4)[Fe(AsO_4)_{1-x}(PO_4)_xF]$ series, the iron(III) arsenate/phosphate obtained after thermal treatment does not exhibit textural porosity, probably due to the absence of the orthorhombic *Imam* $Fe(PO_4)$. The crystal structure of three members of the $(NH_4)[Fe(AsO_4)_{1-x}(PO_4)_xF]$, $x = 0.3$, 0.6, 0.8 members has been refined from single-crystal X-ray diffraction data, together with that of the new $Fe(AsO_4)_{0.7}(PO_4)_{0.3}$ phase, whose textural porosity has been confirmed by TEM measurements and N_2 gas sorption isotherm experiments performed in liquid nitrogen. The spectroscopic and magnetic properties of all the synthesized compounds are also reported in this work.

2. Experimental section

2.1. Hydrothermal synthesis and chemical characterization

The $(NH_4)[Fe(AsO_4)_{1-x}(PO_4)_xF]$ ($x = 0.3$, 0.6, 0.8) series of compounds was synthesized hydrothermally under autogeneous pressure, at 170 °C for five days. The starting reagents were $Fe_2(SO_4)_3(H_2O)_3$ (0.37 mmol), $As_2O_5(H_2O)_3$ [2.7; 1.8 and 0.9 mmol for $x = 0.3$, 0.6 and 0.8, respectively], H_3PO_4 [1.8; 3.7 and 5.5 mmol for $x = 0.3$, 0.6 and 0.8, respectively], HF (57.5 mmol) (handle with caution) and NH_4OH (8.32 mmol) in ca. 30 mL of water with an initial pH of 3. The reaction mixtures were stirred to visual homogeneity and then sealed in a PTFE-lined stainless steel pressure vessel (fill factor 75%). After reaction, slow cooling to room temperature at approximately 30 K h^{-1} was carried out and did not show appreciable change in the pH. In all cases, the resulting product consisted of well-formed light-green single crystals. The composition of the phases was analyzed by inductively coupled plasma atomic emission spectroscopy (ICP-AES) and N-elemental analysis, with the content of fluorine calculated by using a selective electrode. Found: Fe, 25.4; As, 23.9; P, 3.9; N, 6.3; H, 1.7; F, 8.6 for $(NH_4)[Fe(AsO_4)_{0.7}(PO_4)_{0.3}F]$ and requires Fe, 25.5; As, 24.0; P, 4.0; N, 6.4; H, 1.8; F, 8.7. Found: Fe, 27.0; As, 12.9; P, 9.3; N, 6.2; H, 1.6; F, 8.4 for $(NH_4)[Fe(AsO_4)_{0.4}(PO_4)_{0.6}F]$ and requires Fe, 27.2; As, 13.0; P, 9.5; N, 6.3; H, 1.7; F, 8.5. Found: Fe, 28.2; As, 6.7; P, 12.7; N, 6.9; H, 1.8; F, 9.6 for $(NH_4)[Fe(AsO_4)_{0.2}(PO_4)_{0.8}F]$ and requires Fe, 28.4; As, 6.8; P, 12.9; N, 7.0; H, 1.9; F, 9.7. Found: Fe, 30.5; As, 28.7; P, 4.9 for $Fe(AsO_4)_{0.7}(PO_4)_{0.3}$ and requires Fe, 30.7; As, 28.9; P, 5.1.

Single crystals of $(NH_4)[Fe(AsO_4)_{0.7}(PO_4)_{0.3}F]$ were heated under air atmosphere at 465 °C for 40 h in a tubular furnace to obtain the $Fe(AsO_4)_{0.7}(PO_4)_{0.3}$ phase, as brown single crystals. Chemical analyses and IR spectroscopy of this compound indicated the absence of $(NH_4)^+$ and F^- anions in its composition.

The densities of all compounds were measured in a mixture of diiodomethane (CH_2I_2, $\rho = 3.32\ g\ cm^{-3}$) and chloroform (Cl_3CH, $\rho = 1.49\ g\ cm^{-3}$). The values obtained for the $(NH_4)[Fe(AsO_4)_{1-x}(PO_4)_xF]$ ($x = 0.3$ 0.6, 0.8) series are 3.07(1), 2.94(1) and 2.80(1) g cm^{-3}, respectively; in the case of $Fe(AsO_4)_{0.7}(PO_4)_{0.3}$ being of 2.66(2) g cm^{-3}.

2.2. Single-crystal X-ray diffraction experiments and structure studies

Prismatic single crystals of all the compounds, with dimensions given in Table 1, were carefully selected under a polarizing microscope and mounted on a glass fiber. Single-crystal X-ray diffraction data were collected at room temperature on an Oxford Diffraction XCALIBUR2 automatic diffractometer (Mo-$K\alpha$ radiation) equipped with a CCD detector. The data reduction procedures and absorption corrections were carried out by using the diffractometer software [27], and were later performed taking into account the size and the shape of the crystals. If we compare structural data obtained for all the phases belonging to the $(NH_4)[Fe(AsO_4)_{1-x}(PO_4)_xF]$ series presented in this work and considering those with $x = 0$ [24] and 1 [25], it is possible to establish that the volume of the phases shows a linear relation decreasing when the phosphorous content increases in all the members of the series, in good agreement with the minor size of the P atom in comparison with that of the As one (Fig. 1).

The structures were refined using the SHELXL 97 program [28]. The space groups of the title compounds were deduced from the systematic absences observed in the structural determination, taking into account their isostructural character with the phases given in Ref. [24]. For the compound of the series, the fractional atomic coordinates of the $(NH_4)[Fe(AsO_4)F]$ phase [24] were used as a starting structural model (in the $Pna2_1$ space group). However, for the high temperature compound, the atomic coordinates of the $Fe(AsO_4)F$ phase were used (*Imam* space group) [24]. In the refinement procedure of all phases we have considered the fact that there may be two different crystallographic positions for arsenic and phosphorous atoms; however, it was determined that the atoms of phosphorus and arsenic occupy the same position. Thus, their atomic coordinates and temperature factors were refined together, taking into account that the sum of their occupancy factors must be equal to one. In this way, the final overall occupancy factors obtained for the arsenate/phosphate atoms were 0.73(3)/0.27(3), 0.38(3)/0.63(4), 0.18(2)/0.81(4) and 0.69(4)/0.29(3) for $x = 0.3$, 0.6, 0.8 and high

Table 1
Crystal data and details of crystal structure refinement.

Empiric formula	$FeAs_{0.7}P_{0.3}O_4NH_4F$	$FeAs_{0.4}P_{0.6}O_4NH_4F$	$FeAs_{0.2}P_{0.8}O_4NH_4F$	$Fe(AsO_4)_{0.7}(PO_4)_{0.3}$
Formula weight ($g\,mol^{-1}$)	219.73	203.79	195.77	183.78
Dimension	$0.15 \times 0.15 \times 0.25$	$0.12 \times 0.12 \times 0.16$	$0.14 \times 0.14 \times 0.16$	$0.07 \times 0.05 \times 0.03$
Cristal system	Orthorhombic	Orthorhombic	Orthorhombic	Orthorhombic
Space group (N°33)	$Pna2_1$	$Pna2_1$	$Pna2_1$	*Imam*
a (Å)	13.1780(10)	13.0810(10)	13.0329(9)	13.3282(16)
b (Å)	6.5966(6)	6.5341(6)	6.4994(4)	6.5114(5)
c (Å)	10.7972(10)	10.7130(10)	10.6702(6)	10.7031(11)
V ($Å^3$)	938.60(14)	915.67(14)	903.83(10)	928.8(1)1
Z	8	8	8	12
ρ_{obs}, ρ_{calc} ($g\,cm^{-3}$)	3.07(1), 3.11	2.94(1), 2.95	2.80(1), 2.87	2.66(2), 3.94
F(000)	848	796	770	1038
$\mu\,mm^{-1}$	8.324	6.059	4.876	12.774
Radiatión, λ(Mo-*K*α), (Å)	0.71073	0.71073	0.71073	0.71073
Interval *h*, *k*, *l*	$-15 \leqslant h \leqslant 17$, $k \pm 8$, $-13 \leqslant l \leqslant 15$	$-17 \leqslant h \leqslant 12$, $-9 \leqslant k \leqslant 8$, 1 ± 4	$-1-7 \leqslant h \leqslant 11$, $-9 \leqslant k \leqslant 8$, 1 ± 14	$-18 \leqslant h \leqslant 11$, $k \pm 8$, 1 ± 14
R (int)	0.0331	0.0356	0.0346	0.0352
*R*1 [$I > 2\sigma(I)$]	0.0220	0.0262	0.0264	0.0253
*wR*2 [$I > 2\sigma(I)$]	0.0380	0.0469	0.0600	0.0530
*R*1 (All data)	0.0301	0.0400	0.0286	0.0305
*wR*2 (All data)	0.0395	0.0499	0.0609	0.0547
$\Delta_{\rho max}$ y $\Delta_{\rho min}$ ($e\,Å^{-3}$)	0.535, −0.462	0.493, −0.457	0.483, −0.641	1.308, −0.807
G.O.F	0.989	0.943	1.126	1.076

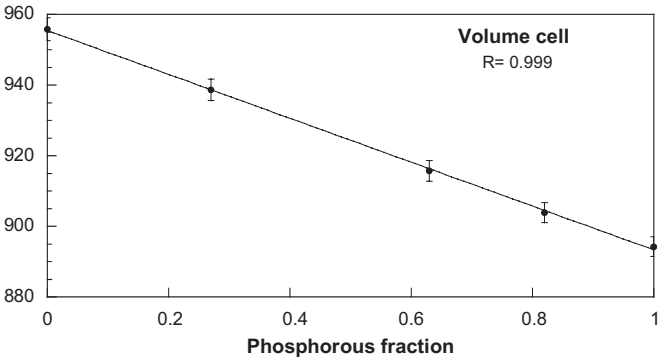

Fig. 1. Evolution of the unit cell volume vs. phosphorous fraction for the $(NH_4)[Fe(AsO_4)_{1-x}(PO_4)_xF]$ ($x = 0.6, 0.8$) series.

temperature phase, respectively. These results are in good agreement with the ICP/AES data analysis (see Table 2).

Finally, a simulation based on the single-crystal structures of all compounds was in excellent agreement with the X-ray powder diffraction data, indicating the presence of pure phases with high crystallinity. Further details on the crystal structure investigation may be obtained from the CCDC upon quoting the depository numbers 420 019, 420 020, 420 021 and 420 022. All structure drawings were made using the ATOMS program [29]. Crystallographic data and details of the refinement procedure, atomic coordinates and selected bond distances and angles are given as Supplementary material. It is important to emphasize the great difference between the experimental ($2.66(2)\,g\,cm^{-3}$) and calculated ($3.94\,g\,cm^{-3}$) density values for high-temperature compound, as the reduction in density is $\frac{2}{3}$, approximately. These discrepancies suggest the existence of a porous nature of the $Fe(AsO_4)_{0.7}(PO_4)_{0.3}$ phase, probably originated by the synthesis procedure. This hypothesis will be corroborated later.

2.3. Physicochemical characterization techniques

The analytical measurements were carried out by using inductively coupled plasma atomic emission spectroscopy on a Perkin Elmer 4110 ZL spectrometer. A SDC 2960 Simultaneous DSC-TGA TA Instrument, under a flow of air with a heating rate of $5\,°C\,min^{-1}$, was used to perform the thermogravimetric analysis up to 800 °C. The calibration in mass was carried out using a standard with known mass; the calibration in temperature was performed with In, Zn, Al and Ag. The DSC calibration was made using a sample of zafire. Time resolved X-ray thermodiffractometry was carried out in air atmosphere on a PHILIPS X′PERT automatic diffractometer (Cu*K*α radiation) equipped with a variable-temperature stage (Anton Paar HTK16) and a Pt sample holder. Transmission electronic microscopy was carried out using a JEOL JSM-6400 instrument. Sorption measurements of N_2 were performed using an ASAP 20010 MICROMETRICS system. IR spectra (KBr pellets) were collected by using a Nicolet FT-IR 740 spectrophotometer in the spectral range 4000–400 cm^{-1}. Diffuse reflectance spectra were registered at room temperature on a Cary 5000 spectrophotometer in the spectral range 2000–210 nm, using a white Teflon to record the base line. A Bruker ESP 300 spectrometer, operating at X band, was used to record the ESR polycrystalline spectra between 4.2 and 300 K. The temperature was stabilized by an Oxford Instrument (ITC 4) regulator. The magnetic field was measured with a Bruker BNM 200 guassmeter and the frequency inside the cavity was determined using a Hewlett-Packard 5352B microwave frequency counter. Magnetic measurements on powdered samples were performed in the temperature range 5.0 or 2.0–300 K, by using a Quantum Desingn MPMS-7 SQUID magnetometer. The applied magnetic field was 0.1 T, a value in the range of linear dependence of magnetization vs. magnetic field, even at 2.0 K.

3. Results and discussion

3.1. Crystal structures

The classical description of the KTiO–(PO_4)-type materials is based on chains of corner sharing octahedra. However, we prefer to describe the structure of the $(NH_4)[Fe(AsO_4)_{1-x}(PO_4)_xF]$ ($x = 0.3$, 0.6, 0.8) series as a three-dimensional framework constructed from corner-sharing FeO_4F_2 octahedra and As/PO_4 tetrahedra. The description allows easier comparison between the KTP crystal structures and that of the derivative high temperature, $Fe(AsO_4)_{0.7}(PO_4)_{0.3}$. Chains, formed by alternating $Fe(1)O_4F_2$ or

Table 2
Occupancy factors.

	As1 occupancy factor	As2 occupancy factor	P1 occupancy factor	P2 occupancy factor
$x = 0.3$	0.7765	0.6993	0.2234	0.3007
Overall, X-ray	⟨0.73(3)⟩		⟨0.27(3)⟩	
Chemical analysis	⟨0.71(2)⟩		⟨0.29(2)⟩	
$x = 0.6$	0.4105	0.3195	0.5895	0.6805
Overall, X-ray	⟨0.38(3)⟩		⟨0.62(4)⟩	
Chemical analysis	⟨0.36(2)⟩		⟨0.64(2)⟩	
$x = 0.8$	0.2249	0.1463	0.7751	0.8537
Overall, X-ray	⟨0.18(3)⟩		⟨0.82(4)⟩	
Chemical analysis	⟨0.18(2)⟩		⟨0.81(2)⟩	
$Fe(AsO_4)_{0.7}(PO_4)_{0.3}$	0.73556	0.64473	0.26444	0.35527
Overall, X-ray	⟨0.69(4)⟩		⟨0.29(3)⟩	
Chemical analysis	⟨0.71(2)⟩		⟨0.29(2)⟩	

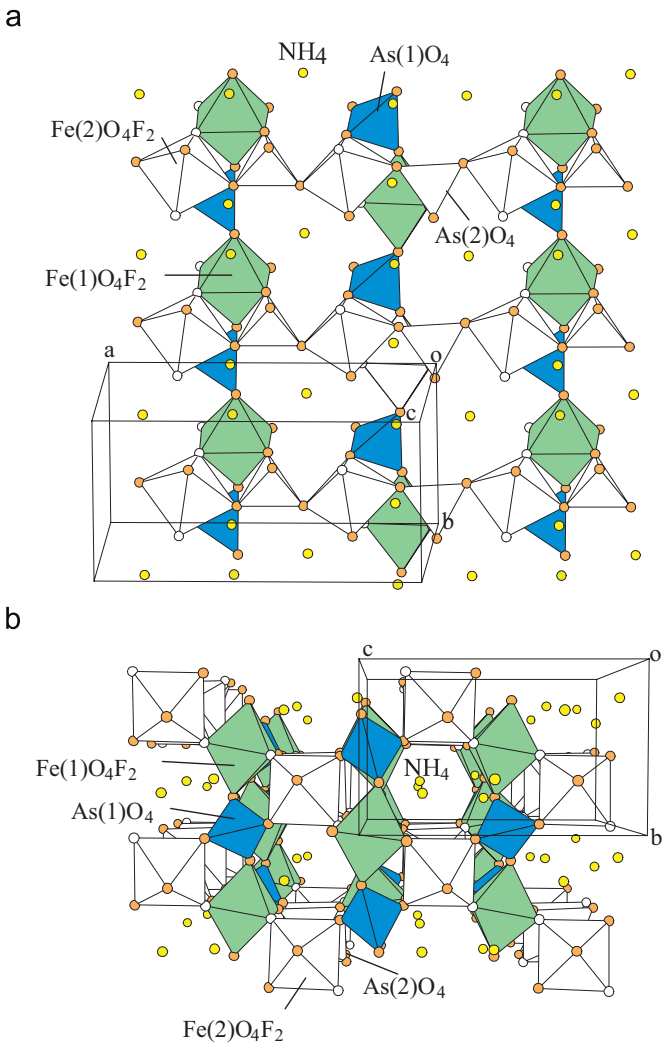

Fig. 2. Polyhedral view of the crystal structure of the $(NH_4)[Fe(AsO_4)_{1-x}(PO_4)_xF]$ ($x = 0.6$, 0.8) series showing (a) the chains and (b) the channels along the |100| direction and |010| directions.

$Fe(2)O_4F_2$ octahedra and $As/P(1)O_4$ or $As/P(2)O_4$ tetrahedra, respectively, are running along the [100] and [010] directions and are linked by a common oxygen vertex (Fig. 2a). The chains are interconnected through the fluoride anions, belonging to the FeO_4F_2 octahedra. This architecture forms six-ring channels along the *a*- and *b*-axes in which the ammonium cations are located in two different crystallographic positions (Fig. 2b). The $(NH_4)^+$ groups compensate the anionic charge of the $[Fe(AsO_4)F]^-$ inorganic skeleton by establishing hydrogen bonds with both the fluorine and oxygen atoms.

For the $(NH_4)[Fe(AsO_4)_{1-x}(PO_4)_xF]$ ($x = 0.3$, 0.6, 0.8) compound, in both octahedra, the iron (III) cations are linked to the oxygen atoms belonging to the (As/PO_4) tetrahedra with a mean Fe–O bond distance of 1.98(5) Å. The hexacoordination is completed by two fluoride anions bonded at a mean bond distance of 1.98(3) Å. The cis- and trans-O–Fe–O bond angles range between 85.0(2)°–100.8(8)° and 171.1(2)°–179.4(2)°, respectively, as expected for slightly distorted octahedral geometry around the iron(III) cations. The arsenic and phosphorous atoms adopt tetrahedral coordination. The mean value of As/P–O bond lengths in $x = 0.3$ phase is 1.64(1) Å. This bond distance is slightly higher than that found for $x = 0.6$ and 0.8, 1.58(7) Å and 1.57(1) Å, respectively, which corresponds to a higher amount of arsenate anion in the $X(1)O_4$ group. The O–As/P–O angles, 109(1)°, in these oxoanions are near to the ideal value expected for a sp^3 hybridization of the central atom in the arsenate and phosphate anions. The bond lengths of XO_4 tetrahedra of the arsenate or/and phosphate phases follow a linear relationship with respect to the amount of arsenic present in the oxoanions.

The mean value of the distortion for the $Fe(1)O_4F_2$, and $Fe(2)O_4F_2$ octahedra and $As/P(1)O_4$ and $As/P(2)O_4$ tetrahedra, from that of an ideal octahedron and tetrahedron, evaluated by the Avnir et al. method [30a,b], is, S(Oh) = 0.0131(3), 0.10(1) and S(Td) = 0.05(1), 0.04(1), respectively, for each polyhedron.

The crystal structure of the high temperature phase, $Fe(AsO_4)_{0.7}(PO_4)_{0.3}$, shows a three-dimensional skeleton constructed from (001) sheets stacked along [001] direction, which are interconnected by chains of alternating $Fe(2)O_6$ octahedra sharing vertices with the $As/P(2)O_4$ tetrahedra. The layers are formed by $Fe(1)_2O_{10}$ edge-sharing octahedra linked by common edges to two $As/P(1)O_4$ tetrahedra, which gives rise to tetrameric units connected to each other by a common oxygen vertex (Fig. 3). The Fe(1) cations belonging to the $Fe(1)O_6$ octahedra are bonded to the O(1) and O(2) atoms from the $As/P(1)O_4$ tetrahedron, and complete the hexacoordination with the O(4) atom belonging to the $As/P(2)O_4$ tetrahedron. The mean Fe(1)–O bond distance is 2.01(3) Å and the cis- and trans-O–Fe(1)–O angles range from 75.3(1)° to 100.8(8)° and from 174.9(2)° to 177.1(1)°, respectively. In the $Fe(2)O_6$ octahedron the metallic cation is bonded to the O(1) and O(3) atoms from the $As/P(1)O_4$ and $As/P(2)O_4$ tetrahedra, respectively, with a mean bond length of 2.004(1) Å. The cis–O–Fe(2)–O angles are in the 86.9(1)°–93.06(11)° range, whereas the trans–O–Fe(2)–O angles have a value of 180°. The distortion of the $Fe(1)O_4F_2$, and $Fe(2)O_4F_2$ octahedra, and $As/P(1)O_4$ and $As/P(2)O_4$ tetrahedra from that of an ideal octahedron and tetrahedron, evaluated by the Avnir et al. method [30a,b], is, S(Oh) = 0.772, 0.075 and S(Td) = 0.587, 0.100, respectively, for each polyhedron.

As already described in the literature [24], both structures are related. While the $(NH_4)[Fe(AsO_4)_{1-x}(PO_4)_xF]$ precursor has a structure formed by two types of FeO_4F_2–AsO_4 perpendicular chains (running along [100] and [010] directions) in the high temperature $Fe(AsO_4)_{0.7}(PO_4)_{0.3}$ compound the chains along the [100] direction remain without modification, and a duplication of the [010] chains takes place, giving rise to the (001) sheets formed by tetrameric units (Fig. 4).

3.2. Thermal study

The thermal decomposition curves of the $(NH_4)[Fe(AsO_4)_{1-x}(PO_4)_xF]$ ($x = 0.3$, 0.6, 0.8) series of compounds reveal a contin-

uous weight loss, with a values of 16.0, 18.0 an 18.5%, for $x = 0.3$, 0.6 and 0.8, respectively, in the temperature range of approximately 553–583 K. This weight loss can be attributed to the elimination of both the ammonium and the fluoride ions in the form of NH_3(g) and HF(g) (the calculated weight loss is in the 16.8–18.9% range). The X-ray powder diffraction patterns of the inorganic residues, obtained at 1073 K, indicate the presence of two different phases. One of them is isostructural with the trigonal iron(III) phosphate [G.E; $P3_121$, $a = 5.02(2)$, $c = 11.23(4)$ Å] [31a] at which the general formula $Fe(AsO_4)_{1-x}(PO_4)_x$ has been assigned. The other one, with the same general formula, is isostructural with the monoclinic iron(III) arsenate [G.E; $P2_1/n$, $a = 5.01(2)$ Å, $b = 8.08(1)$ Å, $c = 7.57(1)$ Å, $\beta = 101.46°$] [31b].

The thermal behavior of the $(NH_4)[Fe(AsO_4)_{1-x}(PO_4)_xF]$ ($x = 0.3$, 0.6, 0.8) series was also studied by time-resolved X-ray thermodiffractometry in air atmosphere. The powder patterns were recorded from room temperature up to 1068 K, in 2θ steps of 0.03° in the range $10 \leqslant 2\theta \leqslant 38.5°$, counting for 2 s per step and increasing the temperature at 288 K min^{-1}. The three members of the series are stable until approximately 573 K, as was also observed from the thermogravimetric measurements. From this temperature, the thermodiffractograms show a temperature range in which a phase transformation is detected. Reaching approximately 738 K different arsenate/phosphates crystallize (see Fig. 5). At high temperatures, the thermodiffractometric behavior is different for every $(NH_4)[Fe(AsO_4)_{1-x}(PO_4)_xF]$ composition. For $(NH_4)[Fe(AsO_4)_{0.7}(PO_4)_{0.3}F]$, the $Fe(AsO_4)_{0.7}(PO_4)_{0.3}$ compound, studied in this work, isostructural to the orthorhombic iron(III) arsenate [S.G.; *Imam*, $a = 13.468(2)$, $b = 6.525(1)$, $c = 10.768(2)$ Å] [24] appears as a pure compound in the 738–813 K range. At higher temperatures, this phase exists together with the $Fe(AsO_4)_{1-x}(PO_4)_x$ trigonal iron(III) arsenate/phosphate [S.G.; $P3_121$, $a = 5.02(2)$ Å, $c = 11.23(4)$ Å] [31a], until 903 K. Since the residue does not appear as a unique phase, the As/P ratios of the phases remain unknown, then the residues will be named as $Fe(AsO_4)_{1-x}(PO_4)_x$. From 903 to 1008 K the trigonal phase exists as the only product, but above 1008 K the $Fe(AsO_4)_{1-x}(PO_4)_x$ monoclinic iron(III) arsenate/phosphate [S.G.; $P2_1/n$, $a = 5.01(2)$ Å, $b = 8.08(1)$ Å, $c = 7.57(1)$ Å, $\beta = 101.46°$] [31b] also crystallizes (see Fig. 5). In the case of $(NH_4)[Fe(AsO_4)_{0.4}(PO_4)_{0.6}F]$, its decomposition yields the $Fe(AsO_4)_{1-x}(PO_4)_x$ orthorhombic iron(III) arsenate, which exists together with the trigonal phase in the 753–828 K range. Above this temperature only appears the trigonal phase that from 1038 K exists together with the monoclinic compound (see Fig. 5). Finally, for the $(NH_4)[Fe(AsO_4)_{0.2}(PO_4)_{0.8}F]$ composition the $Fe(AsO_4)_{1-x}(PO_4)_x$ trigonal phase is the predominant compound in the 435–795 °C range. This phase exists together with the orthorhombic compound [S.G.; *Cmcm*, $a = 5.22(1)$ Å, $b = 7.77(1)$ Å, $c = 6.32(2)$ Å] [32] in the 753–828 K range and with the monoclinic phase in the 1023–1068 K range (see Fig. 5). In the case of the not mixed arsenate/phosphate phases, only the phase $(NH_4)[Fe(AsO_4)F]$ yields the $Fe(AsO_4)$ orthorhombic arsenate in the 723–903 K range, as was reported in a previous work [24].

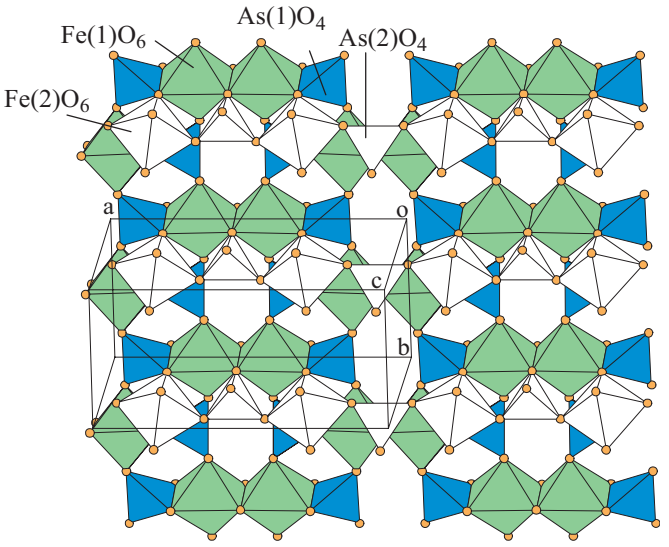

Fig. 3. Polyhedral view of the crystal structure of $Fe(AsO_4)_{0.7}(PO_4)_{0.3}$ showing the layers in the ab-plane.

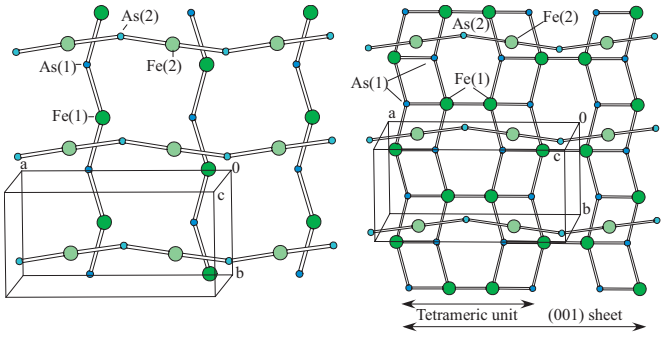

Fig. 4. The relationship betweeen |100| and |010| chains in $(NH_4)[Fe(AsO_4)_{1-x}(PO4)_xF]$ and the |100| chains and the (001) sheets in $Fe(AsO_4)_{0.7}(PO_4)_{0.3}$.

3.3. Transmission electronic microscopy and nitrogen sorption measurements

In order to verify whether the loss of the ammonium and fluoride ions from the $(NH_4)[Fe(AsO_4)_{0.7}(PO_4)_{0.3}F]$ phase causes

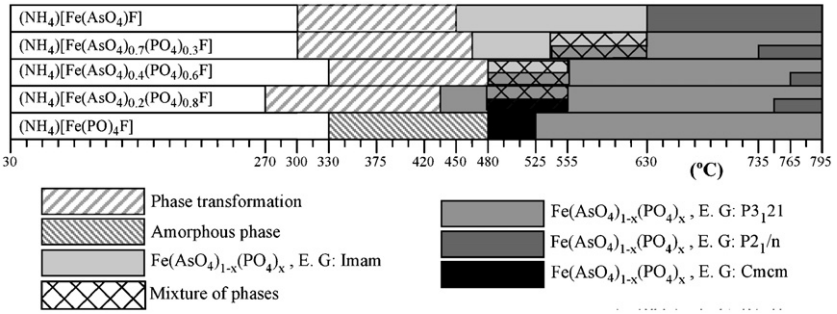

Fig. 5. Schematic representation of the predominance of the different phases present in the thermodiffractograms of the $(NH_4)[Fe(AsO_4)_{1-x}(PO_4)_xF]$ ($x = 0.6$, 0.8) and $Fe(AsO_4)_{0.7}(PO_4)_{0.3}$ phases, at different temperatures.

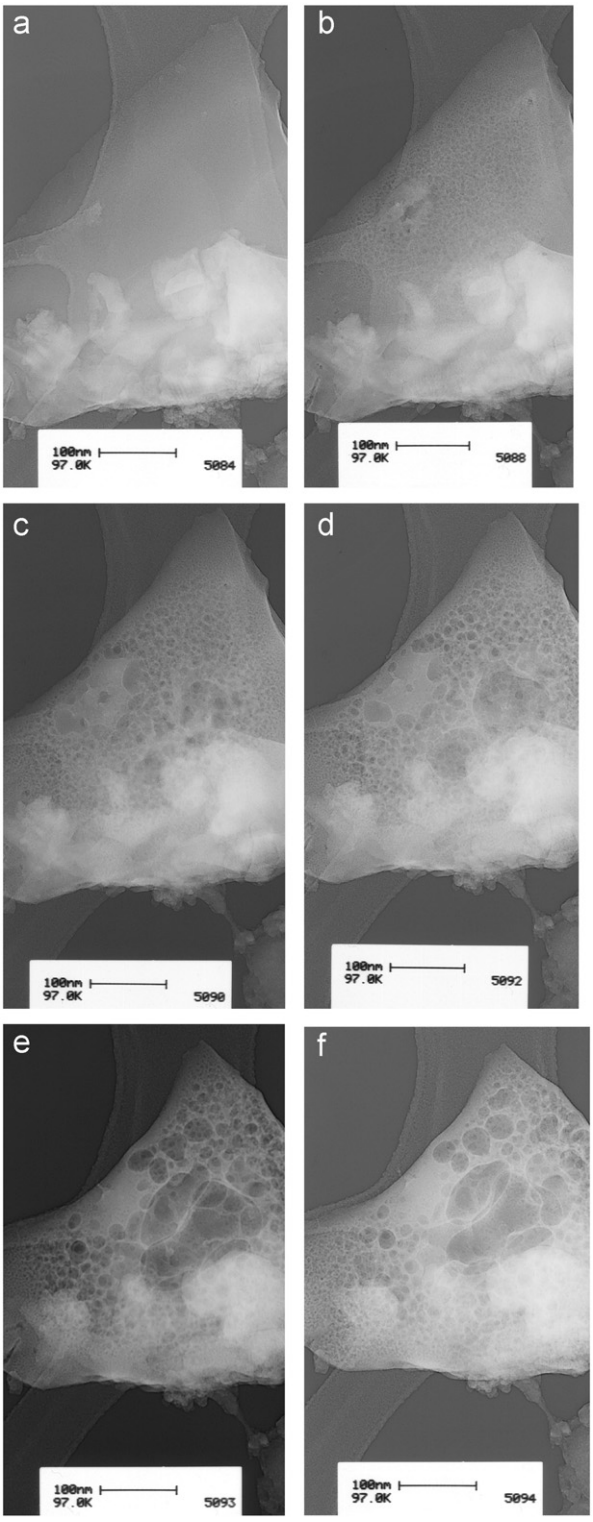

Fig. 6. TEM images of $Fe(AsO_4)_{0.7}(PO_4)_{0.3}$ at different time steps of exposure to the source of electrons: (a) 0, (b) 15, (c) 45, (d) 90, (e) 300, and (f) 600 s, showing the internal and external cavities.

some textural effect on the resulting $Fe(AsO_4)_{0.7}(PO_4)_{0.3}$ compound, as observed in the $Fe(AsO_4)$ phase [24], TEM experiments were carried out. The TEM images taken at different time steps of exposure to a concentrated source of electrons of small single crystals of the $(NH_4)[Fe(AsO_4)_{0.7}(PO_4)_{0.3}F]$ precursor compound, are shown in Fig. 6. The TEM pictures of $Fe(AsO_4)_{0.7}(PO_4)_{0.3}$ show

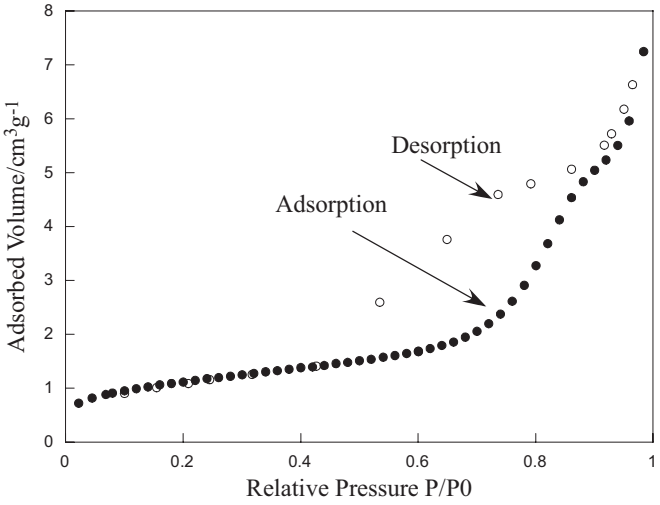

Fig. 7. N_2 adsorption and desorption isotherms measured at 77 K.

that internal and external unconnected cavities are present in the final product. The mean value of cavities is approximately 250 Å. These cavities are generated as a result of the loss of NH_4F from the $(NH_4)[Fe(AsO_4)_{0.7}(PO_4)_{0.3}F]$ precursor. This porosity is possibly formed by the migration of matter from some zones of the $(NH_4)[Fe(AsO_4)_{0.7}(PO_4)_{0.3}F]$ phase to form the $Fe(AsO_4)_{0.7}(PO_4)_{0.3}$ compound. The diffusion of matter could take place across the structural channels of the precursor, duplicating the [010] chains and forming the (001) sheets observed in the $Fe(AsO_4)_{0.7}(PO_4)_{0.3}$ compound (see Fig. 4).

The textural porosity of $Fe(AsO_4)_{0.7}(PO_4)_{0.3}$ was confirmed by gas sorption isotherm experiments, performed in liquid nitrogen. The compound exhibits capacity for N_2 adsorption with a little hysteresis upon desorption (Fig. 7). The measured BET surface area is $3.916(1)\,m^2\,g^{-1}$ and, assuming monolayer coverage by N_2, the Langmuir surface area is estimated to be $5.911(1)\,m^2\,g^{-1}$. This small value can be associated with the existence of unconnected external and internal cavities in the surface of $Fe(AsO_4)_{0.7}(PO_4)_{0.3}$ as was observed from the TEM images. The calculated average pore diameter is approximately 20(1) Å, and corresponds with the value of the superficial pores. The porous nature of $Fe(AsO_4)_{0.7}(PO_4)_{0.3}$, observed by TEM measurements and confirmed by the BET experiments, justifies the reduction of the theoretical density ($3.94\,g\,cm^{-3}$), calculated by X-ray diffraction, until approximately $\frac{2}{3}$, which fits with experimental data [$2.66(1)\,g\,cm^{-3}$].

3.4. IR and UV-Vis spectroscopies

The IR spectra of the $(NH_4)[Fe(AsO_4)_{1-x}(PO_4)_xF]$ ($x = 0.3$, 0.6, 0.8) series show bands above $3180\,cm^{-1}$ that correspond to the stretching vibrational mode of the $(NH_4)^+$ cation. The bending mode of this cation is observed near to $1380\,cm^{-1}$. This signal is not observed for the $Fe(AsO_4)_{0.7}(PO_4)_{0.3}$ phase, confirming the absence of $(NH_4)^+$ groups after thermal treatment. The infrared spectra of all compounds show the characteristic vibrational modes of the arsenate and phosphate oxoanions at typical frequencies [33]. The asymmetrical stretching mode, ν_{as}(As–O), appears at approximately 815, $825\,cm^{-1}$, the ν_{as}(P–O) mode was observed near to 1095 and $1140\,cm^{-1}$. The symmetrical stretching modes, ν_s(As–O) and ν_s(P–O), appear at approximately $730\,cm^{-1}$. Finally, the asymmetrical deformation vibrations, δ_{as}(O–As–O) and δ_{as}(O–P–O), appear near to 510, 465 and 620, $580\,cm^{-1}$, respectively. It is remarkable that the intensity of the vibrational

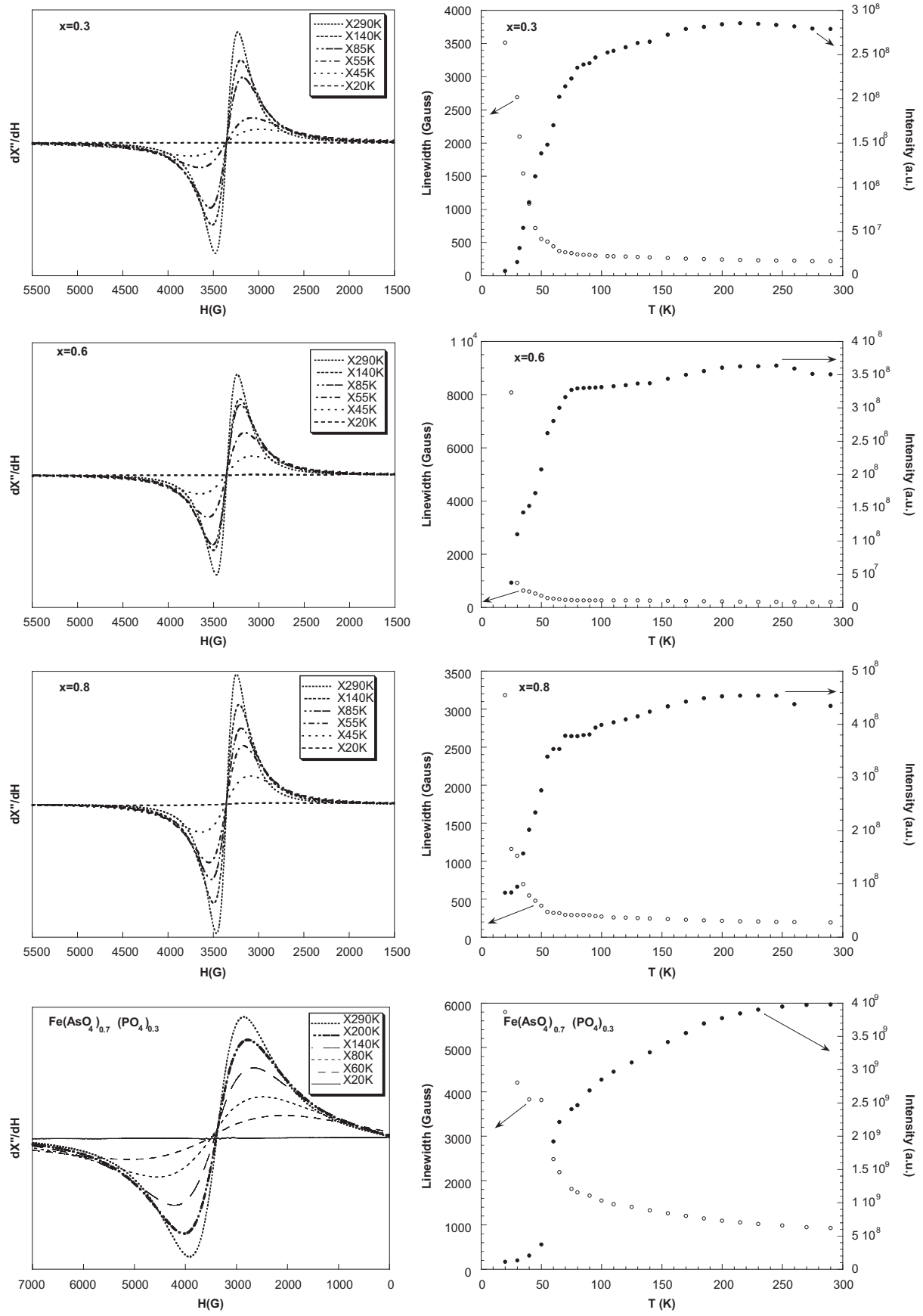

Fig. 8. Powder X-band ESR spectra (left) and temperature dependence of the intensity of the ESR signals and the line width (right).

bands of the arsenate group decreases with the increasing of the ratio of anion phosphate in the composition of the compounds.

The diffuse reflectance spectra of the $(NH_4)[Fe(AsO_4)_{1-x}(PO_4)_xF]$ ($x = 0.3$, 0.6, 0.8) compounds are very similar. In the spectra can be observed four bands at the frequencies ν_1: 13 160, 13 390, 13 475 cm^{-1}; ν_2: 17 830, 17 825, 17 900 cm^{-1}, ν_3: 23 330, 23 375, 23 350 cm^{-1} and ν_4: 25 855, 25 765, 25 725 cm^{-1}, where $x = 0.3$, 0.6, 0.8, respectively. In the spectrum of $Fe(AsO_4)_{0.7}(PO_4)_{0.3}$ is observed a strong absorption in the visible region, in good agreement with its dark color. Consequently of it, only two absorption bands are detected, which correspond to ν_1 at 12 600 and ν_3 at 22 600 cm^{-1}. The intensity of all these bands is weak, as expected for the spin forbidden transitions between the ground state, $^6A_{1g}(^6S)$, and the excited levels $^4T_{1g}(^4G)$; $^4T_{2g}(^4G)$, $^4A_{1g}$, $^4E_g(^4G)$, and $^4T_{2g}(^4D)$ of the Fe(III) d^5-high spin cation, in regular octahedral symmetry [34]. The *Dq* and Racah (*B* and *C*) parameters were calculated by using the Tanabe-Sugano energy expressions [35]. The values obtained for *Dq* are 1160, 1130, 1160 cm^{-1}, where $B = 840$, 795, 790 cm^{-1} and $C = 2985$, 3025, 3089 cm^{-1} for $x = 0.3$, 0.6, 0.8, respectively. These values are in the range habitually found for the iron (III) cation in slightly distorted octahedral environment. The reduction of the *B*-parameter value with respect to that of the free ion (1150 cm^{-1}) in the ammonium compounds is approximately 70%, suggesting an appreciable covalent character in the Fe–O, F chemical bonds. The $Fe(AsO_4)_{0.7}(PO_4)_{0.3}$ compound's Dq and Racah parameters could not be calculated, due to the absence of sufficient spectral bands.

3.5. Magnetic behavior

3.5.1. ESR measurements

The ESR spectra of the $(NH_4)[Fe(AsO_4)_{1-x}(PO_4)_xF]$ ($x = 0.3$, 0.6, 0.8) series and the $Fe(AsO_4)_{0.7}(PO_4)_{0.3}$ compound were recorded on powdered samples at X-band between 4.2 and 300 K (see Fig. 8).

The spectra remain essentially unchanged upon cooling the samples from room temperature to approximately 140 and 200 K for $(NH_4)[Fe(AsO_4)_{1-x}(PO_4)_xF]$ and $Fe(AsO_4)_{0.7}(PO_4)_{0.3}$, respectively. However below these temperatures the line-width of the spectra broadens and loses intensity. The spectra of all the compounds are isotropic with a *g*-value of 1.99(1), which remains unchanged with variation in temperature. This *g*-value is characteristic of octahedrically coordinated d^5-high spin Fe(III) cations [36].

The thermal variation of the intensity and the line-width of the signals, calculated by fitting the experimental spectra to Lorentzian curves, are displayed in Fig. 10. The intensity of the signals, in both the $(NH_4)[Fe(AsO_4)_{1-x}(PO_4)_xF]$ series and $Fe(AsO_4)_{0.7}(PO_4)_{0.3}$ phase, decreases continuously with decreasing temperature from room temperature up to 4.2 K. This result can be associated with the existence of strong antiferromagnetic interactions in all the compounds. The line-width of the ESR signals slightly increases from room temperature up to approximately 50 and 100 K in the $(NH_4)[Fe(AsO_4)_{1-x}(PO_4)_xF]$ and $Fe(AsO_4)_{0.7}(PO_4)_{0.3}$ phases, respectively, as a consequence of the dipolar homogeneous broadening [37]. When the temperature is further decreased, the line-width increases vigorously, which is due to a strong spin correlation [37].

3.5.2. Magnetization measurements

Magnetic measurements of the $(NH_4)[Fe(AsO_4)_{1-x}(PO_4)_xF]$ ($x = 0.3$, 0.6, 0.8) series and $Fe(AsO_4)_{0.7}(PO_4)_{0.3}$ compound were carried out on powdered samples from room temperature to 5.0 and 2.0 K, respectively. The measurements performed at 1000 G in the zero field cooling (ZFC) and field cooling (FC) modes does not show irreversibility for all the members of the $(NH_4)[Fe(AsO_4)_{1-x}(PO_4)_xF]$ ($x = 0.3$, 0.6, 0.8) series. However, irreversibility is observed for the $Fe(AsO_4)_{0.7}(PO_4)_{0.3}$ phase, probably due to some weak ferromagnetic component intrinsic to the sample, detected at low temperatures. Plots of χ_m and $\chi_m T$ curves are given in Figs. 9 and 10, for $(NH_4)[Fe(AsO_4)_{1-x}(PO_4)_xF]$ and $Fe(AsO_4)_{0.7}(PO_4)_{0.3}$, respectively.

The molar magnetic susceptibility, χ_m, of all the compounds increases with decreasing temperature up to approximately 70 and 50 K, temperatures at which the magnetic susceptibility shows a broad or sharp maximum in the case of $(NH_4)[Fe(AsO_4)_{1-x}(PO_4)_xF]$ and $Fe(AsO_4)_{0.7}(PO_4)_{0.3}$, respectively. After these temperatures the susceptibility shows a strong decrease for the series of compounds up to 5.0 K and slightly decreases for the high temperature phase up to approximately 45 K. Finally, the susceptibility again increases in this later phase, suggesting the existence of a spin canting phenomenon. The susceptibility above $T \geqslant 150$ K is described well by a Curie–Weiss law, in all the compounds, with a paramagnetic Curie temperature of approximately −240 and −220 K for $(NH_4)[Fe(AsO_4)_{1-x}(PO_4)_xF]$ and $Fe(AsO_4)_{0.7}(PO_4)_{0.3}$, respectively. These results, together with the continuous decrease observed in the $\chi_m T$ product from 2.90 and 1.98 $cm^3\,K\,mol^{-1}$ for $(NH_4)[Fe(AsO_4)_{1-x}(PO_4)_xF]$ and $Fe(AsO_4)_{0.7}(PO_4)_{0.3}$, respectively, at room temperature, until 0.057 and 0.07 $cm^3\,K\,mol^{-1}$ at 5.0 and 2.0 K, confirm the predominance of strong antiferromagnetic interactions in these compounds.

In order to confirm the existence of a spin canting phenomenon in $Fe(AsO_4)_{0.7}(PO_4)_{0.3}$, ZFC and FC susceptibility measurements at 100 G were carried out. The results are shown in the

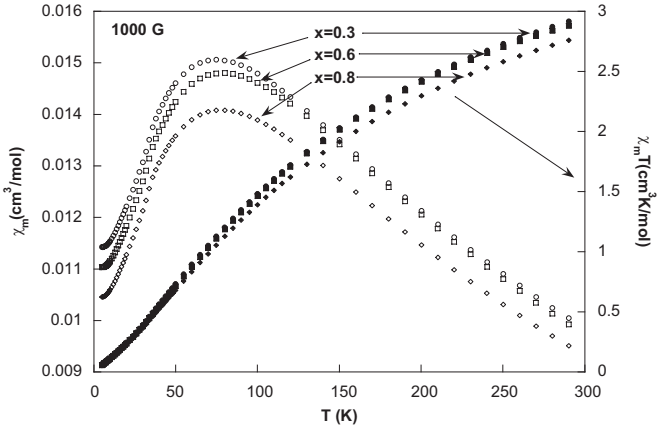

Fig. 9. Thermal evolution of the χ_m and $\chi_m T$ curves at 1000 Oe for the $(NH_4)[Fe(AsO_4)_{1-x}(PO_4)_xF]$ (x = 0.6, 0.8) series.

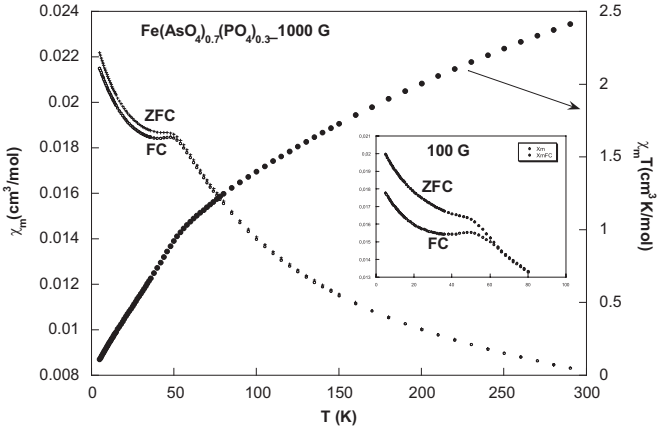

Fig. 10. Thermal evolution of the χ_m and $\chi_m T$ curves at 1000 Oe for $Fe(AsO_4)_{0.7}(PO_4)_{0.3}$. The inset shows the measurements performed at 100 Oe.

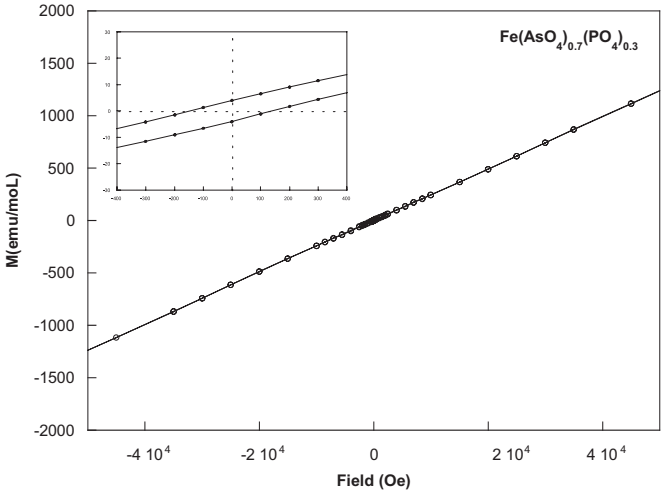

Fig. 11. Hysteresis loop at 2 K for $Fe(AsO_4)_{0.7}(PO_4)_{0.3}$.

inset of Fig. 10. The irreversibility in the magnetic susceptibility for this phase at 100 G starts at 65 K, a temperature that is higher in comparison with that observed, 52 K, at a magnetic field of 1000 G. This fact confirms the existence of a weak ferromagnetic contribution at low temperatures in $Fe(AsO_4)_{0.7}(PO_4)_{0.3}$. In the same way, field-dependent magnetization measurements at 2 K up to 70 KG were recorded for $Fe(AsO_4)_{0.7}(PO_4)_{0.3}$ (Fig. 11). In the low magnetic field region, see inset in Fig. 11, a small hysteresis loop is observed, in which the values of the coercive field and remanent magnetization are 130 Gauss and 5.5 emul mol^{-1}. These results confirm the existence in the $Fe(AsO_4)_{0.7}(PO_4)_{0.3}$ phases of a weak ferromagnetic contribution intrinsic to the sample, probably due to a spin canting phenomenon.

4. Concluding remarks

The $(NH_4)[Fe(AsO_4)_{1-x}(PO_4)_xF]$ $(x = 0.3,\ 0.6,\ 0.8)$ series of compounds has been synthesized by the mild hydrothermal technique, whereas the $Fe(AsO_4)_{0.7}(PO_4)_{0.3}$ phase was synthesized from solid state reaction, in the form of single crystals. Both compounds exhibit a related three-dimensional structure. The ammonium phases are built by two perpendicular chains along the "*x*" and "*y*" axis. The high temperature phase, which was obtained heating single crystals of $Fe(AsO_4)_{0.7}(PO_4)_{0.3}F]$, shows chains formed by tetrameric units, constructed from a duplication of the "*b*" chains, and maintaining invariable those corresponding to the "*a*" axis. $Fe(AsO_4)_{0.7}(PO_4)_{0.3}$ exhibits a textural porosity with a mean value of cavities is approximately 250 Å, and a BET surface area of 5.911(1) $m^2\,g^{-1}$. Magnetic measurements indicate the existence of a global antiferromagnetic ordering, with a weak ferromagnetic component at low temperature, intrinsic to the sample for the $Fe(AsO_4)_{0.7}(PO_4)_{0.3}$ compound.

Acknowledgments

This work has been financially supported by the "Ministerio de Educación y Ciencia" (MAT2007-60400/66737) and the "Gobierno Vasco" (IT-177-07 and IT-312-07). The authors thank the technicians of SGIker, Drs. I. Orue, F.J. Sangüesa and A. Larrañaga, financed by the National Program for the Promotion of Human Resources within the National Plan of Scientific Research, Development and Innovation, "Ministerio de Ciencia y Tecnología" and "Fondo Social Europeo" (FSE), for the magnetic measurements and the X-ray diffraction measurement respectively. T. Berrocal wishes to thank the "Departamento de Investigación y Ciencia del Gobierno Vasco/Eusko Jaurlaritza" for funding.

Appendix A. Supplementary material

Supplementary data associated with this article can be found in the online version at doi:10.1016/j.jssc.2009.01.026.

References

[1] A.K. Cheetham, G. Férey, T. Loiseau, Angew. Chem. Int. Ed. 38 (1999) 3268.
[2] M.E. Davis, Chem. Eur. J. 3 (11) (1997) 1745.
[3] P.B. Moore, in: J. Niagru, P.B. Moore (Eds.), Crystallochemical Aspects of the Phosphate Minerals, Springer, Berlin, 1984.
[4] [a] S. Feng, R. Xu, Acc. Chem. Res. 34 (2001) 239;
[b] J. Yu, R. Xu, Acc. Chem. Res. 36 (2003) 481.
[5] I.D. Williams, M.M. Wum, H.H.-Y. Sung, X.X. Zang, J. Yu, Chem. Commun. (1998) 2463.
[6] J. Chem, L. Li, G. Yang, R.R. Xu, J. Chem. Soc. Chem. Commun. (1989) 1217.
[7] C.N.R. Rao, E.V. Sampathkumaran, R. Nagarajan, G. Paul, J.N. Behera, A. Choudhury, Chem. Mater. 16 (2004) 1441 and references therein.
[8] J.N. Behera, A.A. Ayi, C.N.R. Rao, Chem. Commun. (2004) 968 and the references therein.
[9] R.C. Haushalter, Z. Wang, L.M. Meyer, S.S. Dhingra, M.E. Thompson, J. Zubieta, Chem. Mater. 6 (1994) 3845.
[10] S.-L. Wang, Y.-H. Lee, Inorg. Chem. 33 (1994) 3845.
[11] F. Gagnard, C. Resiner, W. Tremel, Inorg. Chem. 36 (1997) 352.
[12] W.T.A. Harrison, M.L.F. Phillips, A.V. Chavez, T.M. Nenoff, J. Mater. Chem. 9 (1999) 3087.
[13] S. Ekambaram, S.C. Sevov, Inorg. Chem. 39 (2000) 2405.
[14] [a] B. Bazan, J.L. Mesa, J.L. Pizarro, L. Lezama, M.I. Arriortua, T. Rojo, Inorg. Chem. 39 (2000) 6056;
[b] B. Bazan, J.L. Mesa, J.L. Pizarro, A. Goñi, L. Lezama, M.I. Arriortua, T. Rojo, Inorg. Chem. 40 (2001) 5691;
[c] B. Bazan, J.L. Mesa, J.L. Pizarro, M.I. Arriortua, T. Rojo, Mater. Res. Bull. 38 (2003) 3820;
[d] B. Bazan, J.L. Mesa, J.L. Pizarro, L. Lezama, J.S. Garitaonandia, M.I. Arriortua, T. Rojo, Solid State Sci. 5 (2003) 1291;
[e] B. Bazan, J.L. Mesa, J.L. Pizarro, A. Peña, M.I. Arriortua, T. Rojo, Z. Anorg. Allg. Chem. 631 (2006) 2026;
[f] B. Bazan, J.L. Mesa, J.L. Pizarro, L. Lezama, A. Peña, M.I. Arriortua, T. Rojo, J. Solid State Chem. 179 (2006) 1485;
[g] T. Berrocal, J.L. Mesa, J.L. Pizarro, B. Bazán, M. Iglesias, A.T. Aguayo, M.I. Arriortua, T. Rojo, Chem. Commun. (2008) 4738.
[15] S. Chakrabarti, S. Natarajan, Angew. Chem. Int. Ed. 11 (2002) 1224.
[16] G. Férey, Chem. Mater. 13 (2001) 3084.
[17] M. Estermann, L.B. McCusker, C. Baerlocher, A. Merrouche, H. Kessler, Nature (1991) 352.
[18] T. Loiseau, G. Ferey, J. Solid Sate Chem. 111 (1994) 309.
[19] C. Sassoye, T. Loisseau, F. Taulelle, G. Ferey, Chem. Commun. (2000) 943.
[20] C. Sassoye, J. Marrot, T. Loisseau, G. Ferey, Chem. Mater. 14 (2002) 1340.
[21] N. Guillou, Q. Gao, P.M. Foster, J.-S. Chang, M. Nogues, S.-E. Park, G. Ferey, A.K. Cheetham, Angew. Chem. Int. Ed. 40 (2001) 2831.
[22] G. Ferey, J. Fluorine Chem. 72 (1995) 187.
[23] [a] S. Fernandez, J.L. Mesa, J.L. Pizarro, L. Lezama, M.I. Arriortua, R. Olazcuaga, T. Rojo, Chem. Mater. 12 (2000) 2092;
[b] M. Cavellec, D. Riou, J.M. Greneche, G. Ferey, Inorg. Chem. 36 (1977) 2187;
[c] S.-H. Luo, Y.-C. Jiang, S.-L. Wang, H.-M. Kao, K.-H. Lii, Inorg. Chem. 40 (2001) 5381;
[d] B. Bazan, J.L. Mesa, J.L. Pizarro, J.S. Garitaonandia, M.I. Arriortua, T. Rojo, Solid State Sci. 5 (2003) 1291;
[e] P. Zhang, Y. Wang, G. Zhu, Z. Shi, Y. Liu, H. Yuan, W. Pang, J. Solid State Chem. 154 (2000) 368.
[24] B. Bazan, J.L. Mesa, J.L. Pizarro, J. Rodríguez-Fernandez, J. Sanchez-Marcos, A. Roig, E. Molins, M.I. Arriortua, T. Rojo, Chem. Mater. 16 (2004) 5249.
[25] T. Loisseau, Y. Calage, P. Lacorre, G. Ferey, J. Solid State Chem. 111 (1994) 390.
[26] M.E. Hagerman, K.R. Poeppelmeier, Chem. Mater. 7 (1995) 602.
[27] CRYSALIS, version 171.32.5; Oxford Diffraction Ltd.: Oxford, 2007.
[28] Sheldrick, G.M. SHELXL97. Program for the Refinement of Crystal Structures; University of Göttingen: Göttingen, Germany, 1997.
[29] E. Dowty, ATOMS, A computer program for displaying atomic structures, shape sotware, 521 Hidden Valley Road, Kingsport, TN, 1993.
[30] [a] H. Zabrodsky, S. Peles, D. Avnir, J. Am. Chem. Soc. 114 (1992) 7843–7851;
[b] M. Prinsky, D. Avnir, Inorg. Chem. 37 (1998) 5575–5582.
[31] Powder Diffraction File-Inorg and Organic, Files (a) 84–876, (b) 21–410 Pennsylvannia, 1995.
[32] M.E. Arroyo, J.M. Gallardo, M. Amador, Electrochem. Solid State Lett. A 564–A569 (2005) 18.

[33] K. Nakamoto, Infrared and Raman Spectra of Inorganic and Coordination Compounds, Wiley, New York, 1997.
[34] A.B.P. Lever, Inorganic Electronic Spectroscopy, Elsevier, Amsterdam, 1984.
[35] T.Y. Sugano, J. Phys. Soc. Jpn. 9 (1954) 753.
[36] A. Bencini, D. Gatteschi, EPR of Exchange Coupled Systems, Springer, Berlin/Heidelberg, 1990.
[37] [a] H.W. Wijn, L.R. Walker, J.L. Daris, H. Guggenheim, J. Solid State Commun. 11 (1972) 803;
[b] P.M. Richards, M.B. Salamon, Phys. Rev. B 9 (1974) 32;
[c] A. Escuer, R. Vicente, M.A.S. Goher, F. Mautner, Inorg. Chem. 34 (1995) 5707;
[d] T.T.P. Cheung, Z.G. Soos, R.E. Dietz, F.R. Merrit, Phys. Rev. B 17 (1978) 1266.